

Insight into Chemical Reactions from First-Principles Simulations: The Mechanism of the Gas-Phase Reaction of OH Radicals with Ketones

Irmgard Frank* and Michele Parrinello

Max-Planck-Institut für Festkörperforschung, Heisenbergstrasse 1, 70569 Stuttgart, Germany

Andreas Klamt

Bayer AG, 51368 Leverkusen, Germany

Received: December 16, 1997; In Final Form: March 10, 1998

The gas-phase reaction of OH radicals with ketones is investigated using Car-Parrinello molecular dynamics. With a set of dynamical simulations we show that two different reaction mechanisms are important in this system. At higher energies the normal abstraction of hydrogen atoms dominates. In contrast, at low energies the formation of a seven-membered ring is observed that causes an enhancement of the abstraction of the hydrogen atoms at the β carbon atoms.

I. Introduction

The atmospheric reaction of organic compounds with OH radicals determines to a large extent the decomposition of chemical pollutants, and the rate constants for this reaction are taken as a measure for the time of degradation of organic chemicals in the atmosphere. However, the experimental investigation of these reactions and the determination of the reaction rates are difficult and time-consuming.

Among the most common pollutants, ketones play an important role since they are produced in hydrocarbon oxidation processes. The experimental evidence^{1–3} suggests that ketones react with OH radicals in a similar way as alkanes via an abstraction mechanism, resulting in a water molecule and a new radical. However the ketone reactivity differs from that of the alkanes^{1–3} if there are abstractable hydrogen atoms at carbon atoms in the β position to the keto group. In such a case the reaction rate constant is significantly larger than that of the corresponding alkanes (Figure 1). For the estimation of OH rate constants the incremental system by Atkinson⁴ is commonly used. This empirical scheme is based on the assumption that the total reaction rate can be approximated by the sum of the rate constants of individual groups. Within this scheme it turns out that the reactivity of CH, CH₂, and CH₃ groups has to be multiplied by a factor of 4.4 if these groups are located in β position to a keto group.⁴

To explain this observation, the formation of a short-lived six-membered-ring complex has been proposed by Wallington and Kurylo¹ (Figure 2). In this complex the oxygen atom interacts simultaneously with the oxygen atom of the keto group and with the hydrogen atom of the β group. While the OH radical is known to have electrophilic character, for electrostatic reasons one might doubt if such an attractive interaction between the two oxygen atoms is realistic. Thus, a seven-membered complex that involves both atoms of the radical has been proposed alternatively.⁵ The assumption that such a complex initiates the reaction has been successfully used in the calculation of ketone reaction rates with the MOOH method that uses information from semiempirical MO calculations.^{5,6}

We should like to show here that the density-functional-based ab initio molecular dynamics method of Car and Parrinello⁷ (for

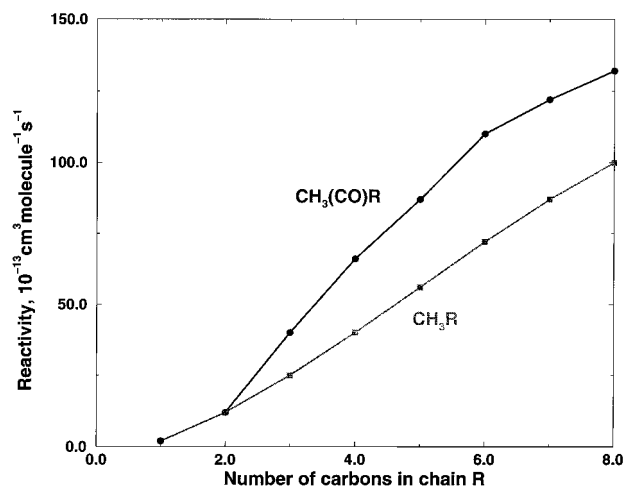


Figure 1. Dependence of rate constants for ketones and alkanes on the length of the carbon chains.¹

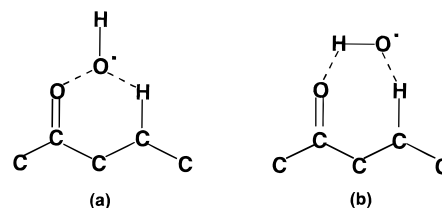


Figure 2. Reactive complexes proposed in the literature: (a) six-membered-ring complex;¹ (b) seven-membered-ring complex.⁵

a review see ref 8) is able to shed new light on the mechanistic details of these radical reactions that involve too many internal degrees of freedom for static investigations of the potential surface. In this quantum-chemical approach the interatomic forces are not preassigned, but are obtained through electronic structure calculations. Thus chemical reactions can take place, since the electronic structure adjusts itself in a self-consistent manner to the evolving atomic positions. Like this, it is possible to determine reaction mechanisms without using any previous assumptions about the reaction pathways. Also information about the relative reaction velocities of different groups can be

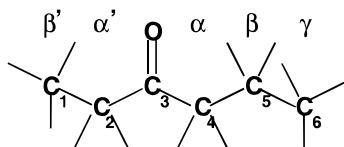


Figure 3. 3-Hexanone.

TABLE 1: Reaction Times and Products from the Simulations

starting geometry	energy [eV]	reaction time [ps]	position
III	0.82	(>2.42)	
III	1.08	1.40	β (C5), hydrogen bond
I	1.19	(>2.42)	
III	1.34	(>2.42)	
II	1.59	(>2.42)	
III	1.60	1.47	α (C4)
III	1.86	2.35	α (C4)
I	1.96	(>2.42)	
III	2.12	(>2.42)	
II	2.37	1.38	α (C4)
III	2.38	1.26	α' (C2)
III	2.63	(>2.42)	
I	2.74	0.69	γ (C6)
III	2.89	0.79	γ (C6)
II	3.14	(>2.42)	
III	3.15	1.97	γ (C6)
III	3.41	(>2.42)	
I	3.52	(>2.42)	
III	3.67	(>2.42)	
II	3.92	(>2.42)	
III	3.93	(>2.42)	

extracted. It should be emphasized that one cannot expect to obtain absolute values for reaction velocities from the calculations, since these quantities depend too sensitively on the barrier heights.

In particular we have studied the reaction of 3-hexanone (Figure 3), since it contains two nonequivalent groups in the β position, CH_2 and CH_3 , whose reactivity is rather different, the CH_2 groups being much more reactive than the CH_3 groups.

II. Theoretical Details

We used Kohn–Sham theory in the local-spin density formulation.^{9,10} The Becke–Lee–Yang–Parr functional^{11,12} was employed. The wave functions were represented by plane waves with a plane-wave cutoff of 70 Ry; the core electrons were described using Troullier–Martins pseudopotentials.¹³ Periodic boundary conditions were employed with a cubic box of 15 au. Unconstrained Car–Parrinello molecular-dynamics runs^{7,8} were performed with a fictitious electron mass of 400 au and a time step of 0.1209 fs (5 au). If after 2.419 ps (10^5 au) no reaction was observed, the run was stopped. The simulations were done for three different starting geometries. The intramolecular bond lengths and angles of these starting geometries are essentially relaxed. However, the intermolecular orientation of the two molecules is not optimized; that is, the starting geometries do not represent local minima of the global potential surface. At the beginning of the run a Maxwell–Boltzmann distribution of atomic velocities was imposed corresponding to different kinetic energies.

III. Results and Discussion

In Table 1 we present a summary of the results obtained. The dependence of the reaction times and the group at which the reaction occurred on the energy of the system is given. The total energy denoted in the table is the sum of the kinetic and

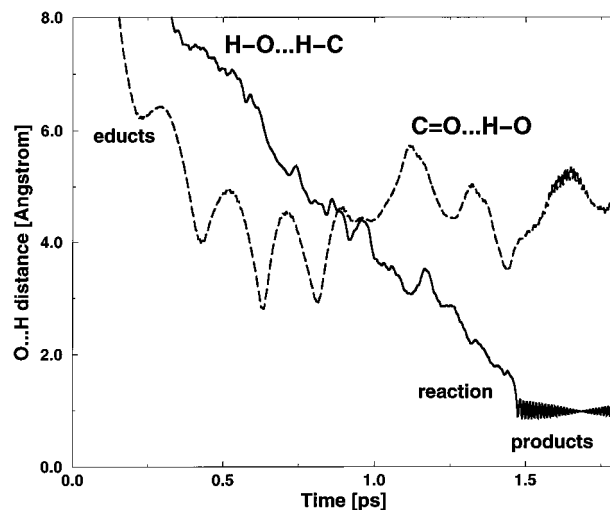


Figure 4. Diagrammatic representation of the high-energy reaction. The plot shows the change of the distance between the radical oxygen atom and the hydrogen atom in the α position ($\text{H}-\text{O}\cdots\text{H}-\text{C}$) and of the distance between the carbonyl oxygen atom and the radical hydrogen atom ($\text{C}=\text{O}\cdots\text{H}-\text{O}$) during the reaction.

the potential energy, $E_{\text{tot}} = E_{\text{kin}} + E_{\text{pot}}$, whereby we define our zero point of energy as the sum of the energies of the two molecules, both independently optimized in the simulation cell. Several observations are in order. First, the results are largely independent of the initial geometry. This is due to the fact that the interaction time that precedes the reaction is long (≈ 1 ps) and the system practically loses memory of the initial geometry. In fact during this time the OH radical collides with the ketone several times and can interact with different hydrogen atoms. This continues until either the molecules drift away from each other or an arrangement is reached that leads to a reaction.

Much more striking is the dependence of the product distribution on the initial kinetic energy of the system. At high kinetic energy only reactions at the α - CH_2 , α' - CH_2 , and γ - CH_3 positions occurred. In order of increasing kinetic energy α , α' , and γ reactions were observed. These high kinetic energy reactions proceed via a simple abstraction mechanism. A typical run in this class of reactions is illustrated in Figure 4. In this particular simulation an abstraction in the α position was observed. We monitor two different quantities: the distance between the radical oxygen atom and an hydrogen atom in the α position ($\text{H}-\text{O}\cdots\text{H}-\text{C}$), and the distance between the hydrogen atom of the radical and the oxygen atom of the carbonyl group ($\text{C}=\text{O}\cdots\text{H}-\text{O}$). It is seen from the decrease in the distance $\text{H}-\text{O}\cdots\text{H}-\text{C}$ that the radical oxygen atom is continuously driven toward the α group. After about 1.5 ps this distance reaches the value of a CH bond length (≈ 1.0 Å), and simultaneously the properties of the molecular vibrations change rather sharply: The high-frequency small amplitude oscillations in the distance $\text{H}-\text{O}\cdots\text{H}-\text{C}$ reflect the formation of a water molecule in a highly excited vibrational state. From the plot it is also seen that the second distance, $\text{C}=\text{O}\cdots\text{H}-\text{O}$, does not fall beyond 2.5 Å throughout the run; that is, there is no hydrogen bond type interaction between the radical and the keto group.

At lower energies (≈ 1.1 eV) we find only a reaction at the β position. This reaction proceeds via a different mechanism, as illustrated in Figures 5 and 6. First a hydrogen bridge between the oxygen atom of the keto group and the hydrogen atom of the radical is formed (Figure 6). Then the dangling oxygen atom approaches one of the hydrogen atoms of the β - CH_2 group and a seven-membered ring as proposed in ref 5

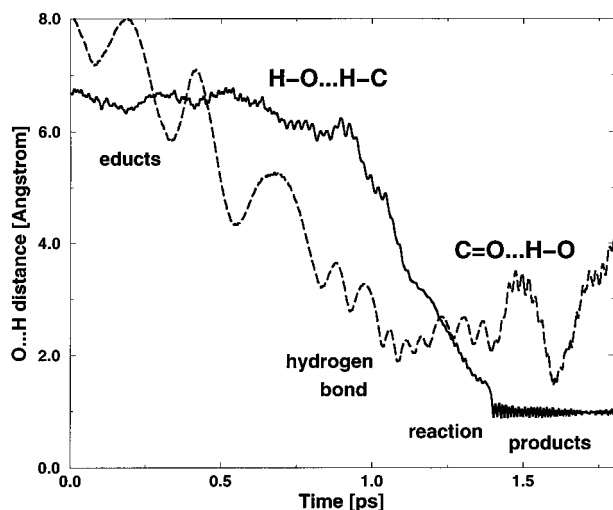


Figure 5. Diagrammatic representation of the low-energy reaction. The plot shows the change of the distance between the radical oxygen atom and the hydrogen atom in the β position ($\text{H}-\text{O}\cdots\text{H}-\text{C}$) and of the distance between the carbonyl oxygen atom and the radical hydrogen atom ($\text{C}=\text{O}\cdots\text{H}-\text{O}$) during the reaction.

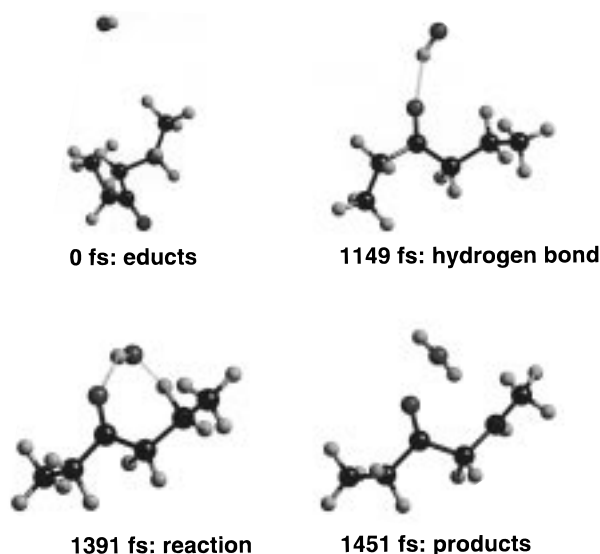


Figure 6. Simulation of the low-energy reaction involving the formation of a hydrogen bond to the keto group.

results. This nonplanar ring is just formed intermediately; it does not correspond to a local minimum on the potential surface. The radical oxygen atom immediately approaches the hydrogen atom of the ketone further to form a chemical bond. The hydrogen bridge to the keto group is broken, a water molecule flies away, and the remaining ketyl radical relaxes (Figure 6). It can be concluded that the formation of the hydrogen bond $\text{C}=\text{O}\cdots\text{H}-\text{O}$ kinetically favors the reaction in the β position. A similar reaction mechanism for the α position that would involve a six-membered ring is not observed.

While the formation of a hydrogen bridge from the keto group to the hydrogen atom of the radical is observed in several runs, there is no indication of an attractive interaction of the two oxygen atoms. Hence we conclude that the complex proposed earlier¹ is not relevant for the reaction.

Recently an addition mechanism has been postulated to explain the negative activation barriers found in the case of aldehydes.¹⁴ From our results such a mechanism is of minor importance for ketones.

We now turn to the discussion of the comparison with the experiments. Clearly the present calculation cannot aim at a quantitative determination of the rate constants and/or the product distribution. On one hand, we have not obtained a sufficiently large set of trajectories to be able to gather enough statistics. On the other hand, present-day theories—and DFT is no exception—cannot achieve the necessary accuracy for such large systems (compare, for example, refs 15, 16). However, on the basis of our limited numerical evidence, we can propose a model for this reaction. We assume that the reaction probability is only a function of the kinetic energy of the system and use our admittedly limited data to model this probability by multiplying our results with the appropriate statistical weight. We estimate the statistical weight by assuming that for the two isolated molecules the equipartition theorem can be applied. Like this, we can explain qualitatively the high probability of the β reaction (66% according to the Atkinson scheme,⁴ 67% according to the MOOH method⁵), since at room temperature the distribution of energies peaks in the region of energies where the reaction is most probable. Similarly, lower values are obtained for the α , α' , and γ reactions (Atkinson: α , 11%, α' , 9%, γ , 3%; MOOH: α , 7%, α' , 3%, γ , 6%), corresponding to the fact that the distribution of energies decreases in the region of energies where these reactions are observed.

We did not observe the analogous reaction for the β' position. The β' reaction should contribute as much as 11% to the total reaction rate according to the Atkinson scheme (MOOH method: 17%); hence, it should be possible to see this reaction in the simulations. The fact that we did not find it should not be overinterpreted. It cannot be taken as an indication either that density-functional theory gives a wrong prediction or that the Atkinson scheme overestimates the weight of this reaction. We cannot obtain enough statistics to prove that a reaction that we did not find could not occur. More statistics and longer dynamics runs would be required to determine the energy dependence of the reaction times for the different reaction mechanisms more precisely.

IV. Conclusions

We have investigated the mechanisms of the reaction of 3-hexanone with OH radicals. The reactions are fast enough to be observed within the time scale of a few picoseconds, and no special constraint method (see for example ref 17) is needed. We find that the reaction products are determined to a large extent by the kinetic energy of the system. Two different reaction mechanisms are observed at different kinetic energies: first, we observe a simple abstraction mechanism. Second, at lower energies we obtain a reaction mechanism that involves the formation of a hydrogen bond between the carbonyl group and the radical. The seven-membered ring that is formed in this way is a purely dynamical phenomenon. The second reaction mechanism is relevant for the hydrogen atoms at β carbon atoms only and explains the enhanced reactivity of this position. To compare our data with the experimental product distribution at 298 K, our results must be weighted with the distribution of energies at that temperature. This comparison shows that density-functional theory is very well suited for the investigation of these systems. To sum up, with Car–Parrinello molecular dynamics it is possible to gain precious insight into chemical reactions without knowing the reaction products in advance. The method presents a valuable tool for determining reaction mechanisms of fast reactions and yields directly a three-dimensional picture of the microscopic processes.

Acknowledgment. Financial support by the Max-Planck-Gesellschaft is gratefully acknowledged. I.F. thanks the Deutsche Forschungsgemeinschaft for her postdoc stipendium.

References and Notes

- (1) Wallington, T. J.; Kurylo, M. J. *J. Phys. Chem.* **1987**, *91*, 5050.
- (2) Dagaut, P.; Wallington, T. J.; Liu, R.; Kurylo, M. J. *J. Phys. Chem.* **1988**, *92*, 4375.
- (3) Atkinson, R.; Aschmann, S. M. *Int. J. Chem. Kinet.* **1995**, *27*, 261.
- (4) Atkinson, R. *Int. J. Chem. Kinet.* **1987**, *19*, 799.
- (5) Klamt, A. *Chemosphere* **1996**, *32*, 717.
- (6) Klamt, A. *Chemosphere* **1993**, *26*, 1273.
- (7) Car, R.; Parrinello, M. *Phys. Rev. Lett.* **1985**, *55*, 2471.
- (8) Parrinello, M. *Solid State Commun.* **1997**, *102*, 107.
- (9) Kohn, W.; Sham, L. J. *Phys. Rev. A* **1965**, *140*, 1133.
- (10) Parr, R. G.; Yang, W. *Density Functional Theory of Atoms and Molecules*; Oxford University Press: Oxford, 1989.
- (11) Becke, A. D. *Phys. Rev. A* **1988**, *38*, 3098.
- (12) Lee, C.; Yang, W.; Parr, R. G. *Phys. Rev. B* **1988**, *37*, 785.
- (13) Troullier, N.; Martins, J. L. *Phys. Rev. B* **1991**, *43*, 1993.
- (14) Taylor, P. H.; Rahman, M. S.; Arif, M.; Dellinger, B.; Marshall, P. *Proc. Intl. Combust. Symp.* **1996**, 497.
- (15) Dupuis, M.; Lester, W. A. *J. Chem. Phys.* **1984**, *81*, 847.
- (16) Soto, M. R.; Page, M. *J. Phys. Chem.* **1990**, *94*, 3242.
- (17) Carter, E. A.; Ciccotti, G.; Hynes, J. T.; Kapral, R. *Chem. Phys. Lett.* **1989**, *156*, 472.